The Plant Cell, Vol. 18, 2443–2451, October 2006, www.plantcell.org

Loading of *Arabidopsis* Centromeric Histone CENH3 Occurs Mainly during G2 and Requires the Presence of the Histone Fold Domain

Inna Lermontova,[a,1] Veit Schubert,[a] Joerg Fuchs,[a] Sabina Klatte,[a] Jiri Macas,[b] and Ingo Schubert[a]

[a] Leibniz Institute of Plant Genetics and Crop Plant Research, D-06466 Gatersleben, Germany
[b] Institute of Plant Molecular Biology, CZ-37005 Ceske Budejovice, Czech Republic

The centromeric histone H3 (CENH3) substitutes histone H3 within the nucleosomes of active centromeres in all eukaryotes. CENH3 deposition at centromeres is needed to assemble the kinetochore, a complex of conserved proteins responsible for correct chromosome segregation during nuclear division. Histones of regular nucleosomes are loaded during replication in S phase, while CENH3 deposition deviates from this pattern in yeast, human, and *Drosophila melanogaster* cells. Little is known about when and how CENH3 targets centromeric loci. Therefore, we determined the location and quantity of recombinant enhanced yellow fluorescent protein (EYFP)-CENH3 in mitotic root and endopolyploid leaf nuclei of transgenic *Arabidopsis thaliana* cells. Our data indicate significant loading of *A. thaliana* CENH3 during G2 (before splitting into sister kinetochores) rather than during the S or M phase of the cell cycle. The histone fold domain of the C-terminal part of CENH3 is sufficient to target *A. thaliana* centromeres. *A. thaliana* EYFP-CENH3 can recognize and target three different centromeric repeats of *Arabidopsis lyrata* but not field bean (*Vicia faba*) centromeres.

INTRODUCTION

Centromeres represent the chromosomal positions of assembly of kinetochore proteins that are responsible for sister chromatid cohesion, chromosome movement, and cell cycle regulation (Allshire, 1997; Choo, 1997; Nicklas, 1997; Amor et al., 2004; Farr, 2004; Henikoff and Dalal, 2005). Kinetochore formation is apparently initiated by incorporation of the histone-like protein centromeric histone H3 (CENH3) (corresponding to human CENP-A) instead of histone H3 into the histone core of centromeric nucleosomes (Howman et al., 2000; Blower and Karpen, 2001). The plant CENH3 homologs share a common core sequence with H3 but diverge as to their N-terminal tails and parts of the C-terminal histone fold domain, in particular the loop 1 region (Malik and Henikoff, 2002). While CENH3 (like the other kinetochore proteins) is highly conserved, centromeric DNA sequences are not (for review, see Houben and Schubert, 2003). Although centromeres are often enriched in tandem repeat arrays and specific retroelements, and many (but not all) of these sequences were found by chromatin immunoprecipitation to be preferentially associated with CENH3, (Vafa and Sullivan, 1997; Warburton et al., 1997; Blower et al., 2002; Zhong et al., 2002; Nagaki et al., 2003; Jin et al., 2004), these sequences are neither indispensable nor sufficient for centromere formation. This was shown for *Drosophila melanogaster* (Karpen and Allshire, 1997; Maggert and Karpen, 2001), human (Amor and Choo, 2002), and plant (Nasuda et al., 2005; Han et al., 2006) chromosomes. Substitution of histone H3 by CENH3 within a proportion of centromeric nucleosomes seems to be essential because depletion of CENH3 causes incorporation of H3 at fly centromeres and defects in chromosome segregation (Blower and Karpen, 2001; Blower et al., 2002). Overexpression of CENH3 yields additional incorporation at noncentromeric positions. While neither centromere activity at ectopic loci nor reactivation of inactive centromeres of dicentric chromosomes was observed in human cells (Van Hooser et al., 2001), overexpression in *Drosophila* revealed functional ectopic kinetochores (Heun et al., 2006).

The timing and mechanism of CENH3 loading at centromeres are still a matter of debate. Deposition during replication of centromeres (signaled by the presence of CENH3 in the parental centromeric nucleosomes), similar to the replication-dependent deposition of other nucleosomal core histones, seems to be reasonable. However, in HeLa cells, synthesis of CENH3 occurs mainly in G2 (Shelby et al., 2000), and, when experimentally restricted to S phase, kinetochore assembly is abolished (Shelby et al., 1997). In *Drosophila* cell cultures, assembly of nucleosomes containing H3 is inhibited during centromere replication, and CENH3 deposition apparently occurs later in the cell cycle (Ahmad and Henikoff, 2001). In fission yeast, CENH3 loading can occur during S phase and in G2-arrested cells (Takahashi et al., 2005). An interesting alternative hypothesis of Mellone and Allshire (2003) assumes that loading of CENH3 is mediated by tension on bipolarly oriented sister centromeres when spindle fibers attach during nuclear division. Correct guidance to and deposition at centromeres of CENH3 during cell cycle stages other than S phase or mitosis is more difficult to explain. Candidates for CENH3-specific assembly factors are Mis6 and

[1] To whom correspondence should be addressed. E-mail lermonto@ipk-gatersleben.de; fax 49-39-482-5137.
The author responsible for distribution of materials integral to the findings presented in this article in accordance with the policy described in the Instruction for Authors (www.plantcell.org) is: Inna Lermontova (lermonto@ipk-gatersleben.de).
www.plantcell.org/cgi/doi/10.1105/tpc.106.043174

Ams2 in fission yeast (Takahashi et al., 2000; Chen et al., 2003). In various organisms, endoreplication cycles omitting G2 and mitosis occur in addition to the mitotic cell cycle and generate endopolyploid nuclei (Brodsky and Uryvaeva, 1977; D'Amato, 1998). Endocycles are faster, need no spindle formation, no chromosome condensation and decondensation, and no breakdown and reconstruction of the nuclear envelope (D'Amato, 1989). If CENH3 is expressed and/or deposited to centromeres during G2 or M phase, endopolyploid nuclei should not harbor more CENH3 than 2C nuclei.

To elucidate the cell cycle stage and the reason for centromere specificity of CENH3 deposition in *Arabidopsis thaliana*, nuclei from various tissues of plants transgenic for enhanced yellow fluorescent protein (EYFP)-tagged *A. thaliana* CENH3 were studied as to the presence, localization, and quantity of fluorescence signals. The results, in agreement with those obtained after immunostaining with anti-CENH3 antibodies, indicate that most CENH3 is loaded in the absence of ongoing replication (as in fly and human cells) (i.e., during G2). Endopolyploid nuclei up to the 8C level revealed only little more CENH3 than 2C nuclei. Furthermore, EYFP-CENH3 of *A. thaliana* seems to be deposited at all centromeres of *Arabidopsis lyrata*, possessing three different types of centromeric repeats on different chromosomes, each with a different degree of similarity to the *A. thaliana* centromeric sequence repeat (Berr et al., 2006). Moreover, after transformation with constructs linking either the N- or C-terminal part of CENH3 with EYFP, only nuclei transgenic for the latter construct displayed fluorescence signals at centromeric positions.

RESULTS

In Most Nuclei, CENH3 Colocalizes Exclusively with Centromeric Regions/Repeats

A. thaliana plants (2n = 10) constitutively expressing EYFP-tagged *A. thaliana* CENH3 fusion protein (EYFP-CENH3) were analyzed for incorporation of CENH3 into the centromeric regions of meristematic and endoreduplicated nuclei from roots and young and mature leaves, respectively. Flow cytometric analysis revealed almost 100% of living leaf nuclei with EYFP-CENH3 fluorescence. Most living root tip nuclei, analyzed by fluorescent microscopy, displayed up to 10 signal foci (Figures 1B and 1C). During mitosis, EYFP-CENH3 was localized exclusively at the presumed centromeres (Figures 1D and 1E), suggesting that expression of recombinant CENH3 in the selected transgenic lines is not above the physiological level (Shelby et al., 1997; Irvine et al., 2004). Protein gel blot analysis revealed a single band of ~25 kD corresponding to endogenous CENH3 in the control and transgenic lines, while no fusion protein was detectable (Figure 2). Also with anti-green fluorescent protein (GFP) that recognizes EYFP, EYFP-CENH3 was not detectable on protein gel blots. This indicates an expression level of EYFP-CENH3 that is much lower than that of endogenous CENH3.

Since EYFP fluorescence bleaches very fast, we performed immunostaining experiments with anti-GFP antibodies and found fluorescence signals at centromeres during interphase and mitosis (Figures 1F to 1K). In late G2, prophase, and metaphase nuclei, double signals with a distance between the single spots of up to 0.5 μm appeared (Figures 1G, 1H, and 1K). Immunosignals for CENH3 were observed in 93.1% of 250 root tip nuclei, in most of them exclusively at chromocenters.

Immunosignals for EYFP-CENH3 occur at the edges of fluorescence in situ hybridization (FISH) signals for centromeric ~180-bp repeats that in turn occupy part of the 4′,6-diamidino-2-phenylindole (DAPI)-positive chromocenters (Figure 1J). In case of double immunosignals, these are connected by centromere-specific FISH signals (Figure 1K).

Within meiotic nuclei, immunofluorescence signals were localized at the core of bright DAPI-stained heterochromatic regions of leptotene, pachytene, and diakinesis chromosomes and occasionally less dense along the chromosome arms. In leptotene, up to 10 separate signals were found, while in pachytene, the signals of homologous chromosomes (and sometimes all signals) were fused. During diakinesis, five double signals were localized on centromeres (Figures 1L to 1N). The intensity of EYFP-CENH3 immunosignals per nucleus during meiotic prophase (pachytene) is comparable ($P = 0.263$) to that of mitotic prophase nuclei.

Endoreplication Does Not Proportionally Increase the Amount of CENH3

Nuclei isolated from fully developed leaves of EYFP-CENH3 transformants were sorted according to their ploidy level (2C, 4C, 8C, and 16C) and immunostained using antibodies against GFP (Figures 3A and 3C). Compact fluorescent signals were observed in 2C, 4C, and most of 8C nuclei, while in 16C nuclei, the signals were often less compact and split into smaller foci. The total volume of all fluorescence signals per nucleus was measured on optical stacks of labeled nuclei by three-dimensional (3D) microscopy. Assuming that the total volume of immunosignals directly reflects the amount of EYFP-CENH3 within a nucleus, no increase ($P = 0.844$) in EYFP-CENH3 content from 2C to 8C endopolyploidy level was found (Table 1). The increase ($P < 0.05$) measured in 16C nuclei could be due to decreased signal compaction (Figures 3A and 3C). The average EYFP-CENH3 immunosignal volume of 16 randomly selected nuclei of different sizes from squashed leaves was $1.19 \pm 0.12\ \mu m^3$, similar as in flow sorted 2C to 8C nuclei (Table 1). When EYFP-CENH3 fluorescence was measured by flow cytometry, the relative fluorescence intensity increased with ploidy level but reaches only 28.7% of the value expected in 16C nuclei if CENH3 content doubled along with the DNA content. To exclude that during endocycles centromeric ~180-bp tandem repeats colocalizing with (Talbert et al., 2002) and binding to CENH3 (Nagaki et al., 2003) remain underreplicated as in some polytene chromosomes (Nagl, 1978) and therefore that CENH3 loading is not required, FISH signal volumes were determined for isolated leaf nuclei of 2C to 16C level. In contrast with the CENH3 signal volumes, the FISH signal volumes in 2C, 4C, and 16C nuclei were found to be proportionally increased with the DNA content (Table 1). Surprisingly, in repeated experiments from 4C to 8C level, no proportional increase of centromeric FISH signals could be detected. However, when considering the histogram peak positions of 2C

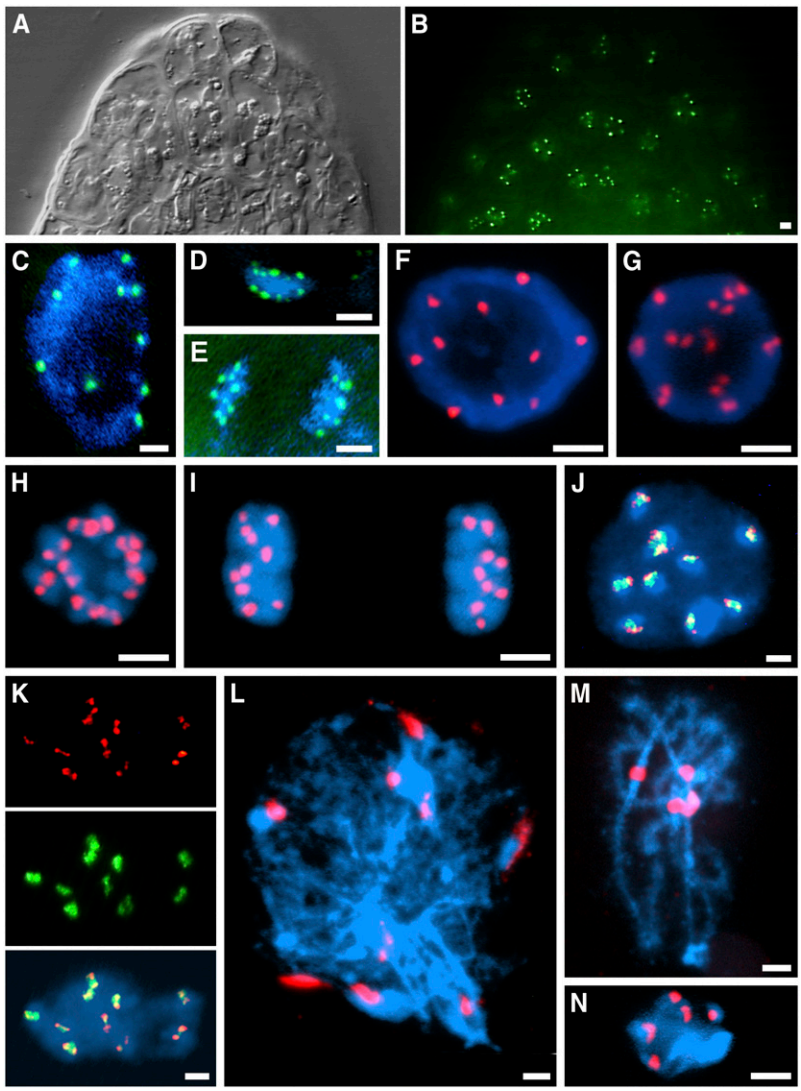

Figure 1. Localization of EYFP-CENH3 in Nuclei of Transgenic *A. thaliana* Plants.

(A) Differential interference contrast image of an *A. thaliana* root tip.
(B) The same root tip with EYFP signals.
(C) to **(E)** EYFP signals in living interphase **(C)**, metaphase **(D)**, and anaphase **(E)** nuclei.
(F) to **(K)** Immunostaining with anti-GFP antibodies (red) and/or FISH with centromeric ~180-bp repeats (green) on meristematic root tip nuclei: early G2 **(F)**, late G2 **(G)**, prometaphase **(H)**, telophase **(I)**, early G2 showing positional coincidence of immunosignals for EYFP-CENH3, FISH signals for the ~180-bp centromeric repeat, and bright DAPI-stained chromocentres **(J)**, and late G2 showing colocalization of EYFP-CENH3 double dots (red) with centromeric ~180-bp repeats (green) **(K)**.
(L) to **(N)** Immunostaining of EYFP-CENH3 on meiotic chromosomes: leptotene **(L)**, pachytene **(M)**, and diakinesis **(N)**. DNA is counterstained with DAPI (blue). Bars = 2 μm.

to 16C nuclei after DNA staining (Figure 4A), no underreplication that could explain the low increase in CENH3 content was detectable. Since CENH3 amounts do not increase proportionally with the C values and with the amounts of centromeric repeats in endoreplicated nuclei, most of CENH3 is not loaded to centromeres during S phase of endoreduplicating nuclei. Because no significant underreplication was detectable, an obvious difference to mitotic S phase is not apparent.

CENH3 Is Loaded to Centromeres Mainly during G2 but Not during Mitosis

To test whether loading of CENH3 may occur during mitosis (e.g., due to spindle-mediated tension) (Mellone and Allshire, 2003), the volumes of CENH3-specific signals were determined for prophase and telophase nuclei from root tips. No significant differences as to the relative amounts of CENH3 were detectable

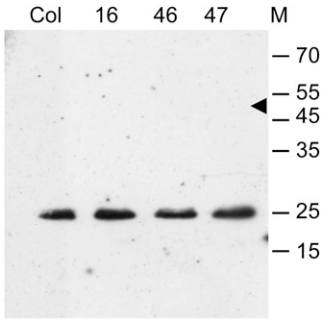

Figure 2. Protein Gel Blot Analysis of Flower Buds from *A. thaliana* Wild-Type (Columbia) and Transgenic Lines (16, 46, and 47) Expressing the EYFP-CENH3 Fusion Protein Using Antibodies against *A. thaliana* CENH3.

Only endogenous CENH3 yielded a band of ~25 kD. The larger recombinant protein (~51 kD, arrowhead) remains below the level of detection; this was also true when anti-GFP antibodies were applied.

between prophase and telophase nuclei (Table 2). This excludes a major tension-mediated CENH3 deposition during mitosis. Large G2 root tip nuclei (4C) with doubled fluorescence signals revealed similar total signal volumes as observed in prophase nuclei (Table 2) but much larger ones than found in 2C nuclei. For some nuclei of these different types, in parallel to signal volume measurement, the intensity of EYFP-CENH3 immunofluorescence signals was determined and yielded a similar ratio.

To confirm that EYFP-CENH3 signal ratios reflect the loading of CENH3 to centromeres, indirect immunostaining using antibodies against *A. thaliana* CENH3 was applied to *A. thaliana* wild-type nuclei. The signal volumes and signal intensities in presumed G1 and G2 root tip nuclei with up to 10 signals were nearly identical, whereas in late G2 nuclei with 20 signals, both values were about doubled (Figure 4B). Thus, our data indicate that most of CENH3 is loaded during (late) G2 rather than during S phase or mitosis.

The C-Terminal Part of CENH3 Is Responsible for the Recognition of Centromeres Even When They Differ as to Their Repeat Composition

To test whether the highly variable N-terminal part of CENH3 or rather the C-terminal part, which differs from H3 mainly as to the composition of the so-called loop 1 region, is responsible for recognition of centromere positions, DNA fragments encoding both parts were separately fused with EYFP and used to transform *A. thaliana*.

While the N-terminal part yielded fluorescence equally distributed over the entire nuclei (Figure 5B), the C-terminal part was targeted to chromocenters (Figure 5C). Thus, the C-terminal histone fold domain including the variable loop 1 region is apparently sufficient to direct the CENH3 to centromeres even when its N-terminal part is absent. Since computer analysis of *A. thaliana* CENH3 did not reveal any nuclear localization signal, CENH3 might be transported to nuclei by a carrier (or, in case of fragments, even via diffusion).

The CENH3 protein is highly conserved within the genus *Arabidopsis* (Cooper and Henikoff, 2004). *A. thaliana* and *A. lyrata* share 93% of amino acid residues of the C-terminal region and 77% of the N-terminal region (Figure 5A). To test whether *A. thaliana* CENH3 can recognize the three different types of centromeric repeats of *A. lyrata* ($2n = 16$), young seedlings of *A. lyrata* were transiently transformed with the corresponding construct of *A. thaliana*. Transformed *A. lyrata* nuclei showed up to 16 fluorescence signals (Figure 5D). This indicates that all *A. lyrata* centromeres are recognized irrespective of their repeat composition. However, *A. thaliana* CENH3 did not target the centromeres of a species as distantly related as *Vicia faba.* After transformation of hairy roots with the EYFP-CENH3 construct,

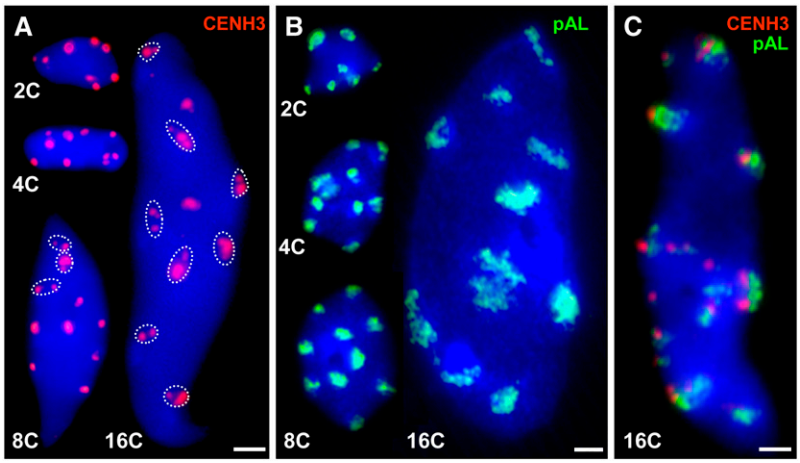

Figure 3. Number and Appearance of EYFP-CENH3–Specific Immunosignals and Centromere-Specific FISH Signals in *A. thaliana* Nuclei of Different Endopolyploidy Levels.

Sorted nuclei after immunofluorescence labeling of EYFP-CENH3 **(A)**, FISH detection of centromeric ~180-bp repeats **(B)**, and the combination of both in a 16C nucleus **(C)**. DNA is counterstained with DAPI (blue). In 2C to 8C nuclei, immunofluorescence and FISH signals are mainly compact, while in 16C, signals were often disperse or split into smaller foci (circled). Bars = 2 μm.

Table 1. Proportions of EYFP-CENH3 Immunosignals (Obtained with GFP-Cy3 Antibodies) and ~180-bp Centromeric Repeat (pAL) FISH Signals within Leaf Nuclei Isolated from EYFP-CENH3 Transgenic *A. thaliana* and Sorted According to Their Endopolyploidy Level ± SE

	EYFP-CENH3				pAL			
Ploidy	Nuclei No.	Nuclei Volume (μm^3)	CENH3 Signal No.	CENH3 Volume (μm^3)	Nuclei No.	Nuclei Volume (μm^3)	pAL Signal No.	pAL Volume (μm^3)
2C	10	22.55 ± 2.98	7–10	1.22 ± 0.15	10	27.04 ± 2.22	8–12	3.42 ± 0.23
4C	13	38.02 ± 3.41	6–11	1.11 ± 0.19	10	58.08 ± 4.11	7–11	7.25 ± 0.52
8C	11	83.55 ± 8.41	7–13	1.25 ± 0.20	20	116.74 ± 10.03	9–14	9.33 ± 0.55
16C	11	213.9 ± 20.5	9–25	3.19 ± 0.55	10	322.81 ± 33.2	10–17	29.22 ± 3.71

EYFP fluorescence was found only within the cytoplasm (Figure 5E).

DISCUSSION

CENH3 Locates Mainly at One Compact Centromere Domain per Chromosome until Sister Centromeres Split in Late G2 or Disperse in Highly Endopolyploid Nuclei

In contrast with previous investigations on *A. thaliana* CENH3 (Talbert et al., 2002; Fang and Spector, 2005), we combined in vivo, in situ, and flow cytometric studies. This facilitated localization and quantification of EYFP-CENH3 on chromosomes as well as in interphase nuclei of defined ploidy level. We confirmed CENH3 localization mainly at distinct centromeric regions on mitotic and on meiotic chromosomes and by positional overlap with centromere-specific FISH signals also in interphase nuclei. Double dots in G2 and prophase nuclei indicate that centromere-flanking regions of sister chromatids with H3-containing nucleosomes might be cohesive until the onset of anaphase, while sister regions that contain CENH3 and form the basis of kinetochores (Henikoff and Dalal, 2005) are separated already before prophase. The similarity of EYFP labeling patterns with signals obtained after immunostaining with anti-GFP and anti-CENH3 antibodies (Talbert et al., 2002; this study) and the protein gel blot data for wild-type and EYFP-CENH3 transformants indicate that in EYFP-CENH3 transformants, expression of CENH3 was within the physiological range and overexpression can be excluded. The dispersion of compact signals yielding smaller signal foci previously observed in root tip nuclei (Talbert et al., 2002) or in some large epidermal nuclei (Fang and Spector, 2005) was restricted in our study mainly to endopolyploid nuclei of ≥16C, which also showed dispersion of sister centromeres after FISH with centromeric repeats (Schubert et al., 2006).

No Evidence for CENH3 Loading Proportional to Replication or during Mitosis

During endocycles, the *Arabidopsis* genome is fully replicated. Only a weak increase of CENH3 content compared with the DNA content was evident from 2C up to the 8C level. This observation indicates that the main CENH3 deposition does not occur during replication. Since early and late mitotic stages revealed the same

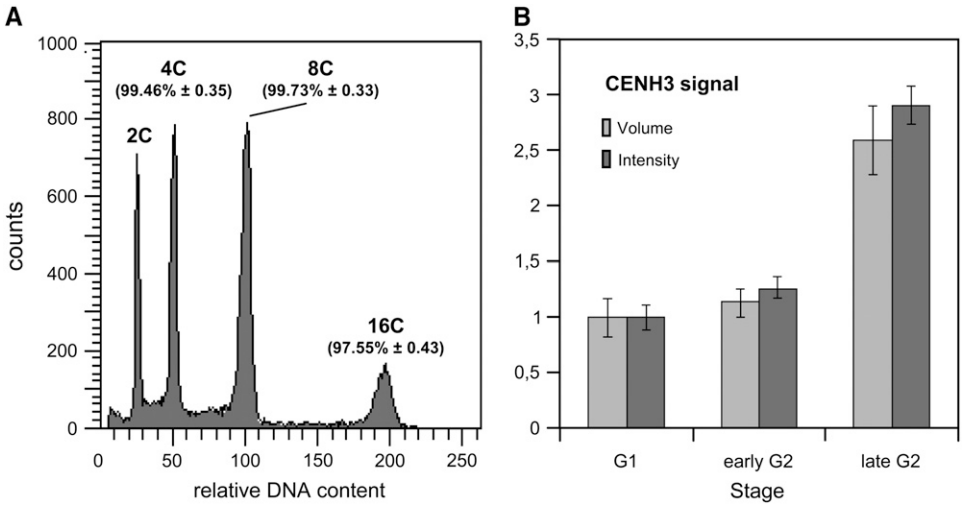

Figure 4. DNA Increase at Various Endopolyploidy Levels and Relative Proportions of CENH3 in *A. thaliana* Wild-Type Nuclei.

(A) Histogram showing the relative DNA content (±SE) of leaf nuclei after DAPI staining and flow cytometric analysis ($n = 10$) for distinct ploidy levels as percentages of the predicted amounts for a complete duplication of the genome per endocycle.

(B) Relative proportions of CENH3 immunosignals (obtained with CENH3-rhodamine antibodies) in presumed early G2 and late G2 versus G1 nuclei (see Table 2) of *A. thaliana* root tip meristems expressed as signal volumes and signal intensity (±SE), respectively ($n = 10$).

Table 2. Proportions of EYFP-CENH3 Immunosignals (Obtained with GFP-Cy3 Antibodies) in G2 and Prophase (4C) versus G1 and Telophase (2C) Nuclei of *A. thaliana* Root Tip Meristems Transgenic for EYFP-CENH3 (Line 36) ± SE

Stage[a]	Nuclei No.	Nuclei Volume (μm^3)	CENH3 Signal No.	CENH3 Volume (μm^3)	CENH3 of Nuclear Volume (%)
G1	10	37.10 ± 3.75	10	0.90 ± 0.06	2.43
Early G2	10	117.97 ± 12.20	10	1.01 ± 0.12	0.86
Late G2	10	120.79 ± 9.57	20	1.84 ± 0.13	1.52
Prophase	19	51.32 ± 3.54	20	1.94 ± 0.13	3.78
Telophase	24	23.00 ± 1.88	10	0.97 ± 0.09	4.21

[a] Of spheric nuclei with large nucleoli, typical for meristems, the largest ones are considered to be in G2 and the smallest ones in G1. Due to their huge nucleoli, their volumes are much bigger and the CENH3 proportion of the nuclear volume smaller than the corresponding values for prophase and telophase nuclei. Because double signals occurred on pro- and metaphase chromosomes, we address large interphase nuclei harboring double signals as late and those with up to 10 single signals as early G2 nuclei.

relative amount of CENH3, although prophase nuclei showed an approximately twofold CENH3 content compared with 2C nuclei, spindle-mediated tension at centromeres does not cause significant CENH3 loading immediately during mitosis. However, we cannot exclude a mark set by tension that acts (much) later in the daughter cells. Obviously most of CENH3 becomes loaded before nuclear division. Large nuclei from squashed root tips with double anti-CENH3 immunosignals (late G2) also have a doubled fluorescence intensity compared with nuclei of similar size with up to 10 single signals (early G2) (Figure 4B). The same was true for anti-GFP immunosignals (data not shown). Therefore, most of CENH3 loading apparently takes place in G2 nuclei, during or immediately before splitting of sister centromere domains. It has been shown that several genes that are regulated during G2 contain binding motives for the E2F family of transcription factors in their promoter regions (Ishida et al., 2001; Polager et al., 2002; Ren et al., 2002). Computer analysis of the presumed promoter region of *A. thaliana* CENH3, using the NSITE program (available through SoftBerry, http://www.softberry.com/berry.phtml?topic=promoter), revealed two putative E2F1 binding sites (GCGGGAAA at −163 and −115 bp from the ATG start), suggesting CENH3 expression during G2. Also in human cells, CENH3 becomes preferentially expressed in G2 (and downregulated upon DNA damage-mediated cell cycle

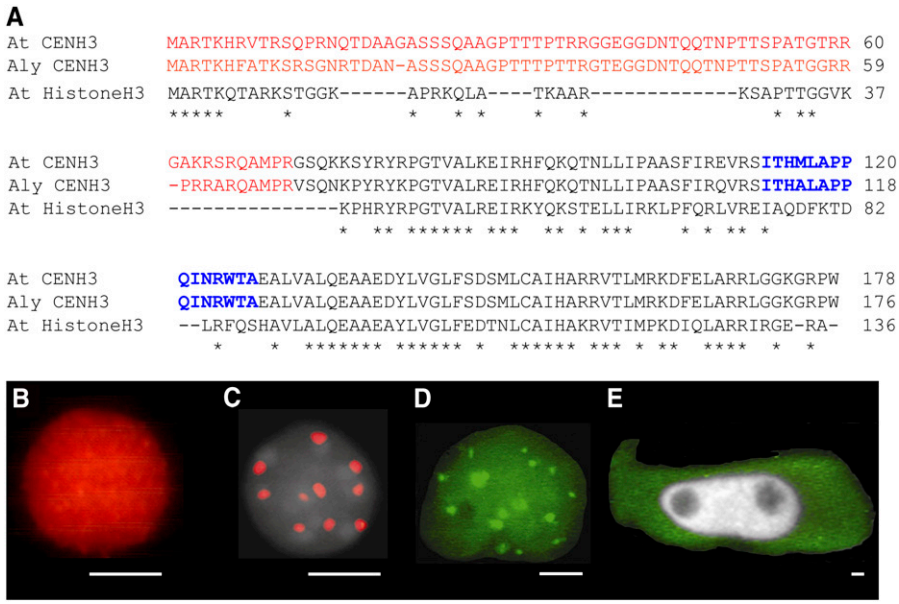

Figure 5. CENH3 sequences and *A. thaliana* CENH3 Localization in Nuclei of Transgenic *A. thaliana*, *A. lyrata*, and *V. faba* Cells.

(A) Sequence alignment of At CENH3, Aly CENH3, and At Histone H3. The N-terminal parts are in red, C-terminal histone fold domain is in black, loop1 regions are in blue, and asterisks indicate sequence identity.

(B) and **(C)** Immunolocalization of N-terminal **(B)** and C-terminal **(C)** parts of *A. thaliana* CENH3 fused with EYFP by anti-GFP antibodies (red) and counterstaining with DAPI (gray).

(D) In vivo fluorescence (16 spots) in an *A. lyrata* nucleus transiently transformed with the EYFP-CENH3 construct.

(E) In vivo fluorescence (green) of a *Vicia faba* hairy root cell transgenic for EYFP-CENH3; the nucleus (gray) remained unlabeled. Bars = 2 μm for **(B)** to **(E)**.

arrest) when intact *cis*-acting elements in its promoter are present (Badie et al., 2000). These observations suggest that expression during G2 might be a conserved feature of CENH3. Albeit driven by the constitutive 35S promoter, loading of EYFP-CENH3 occurs preferentially during G2. Expression and deposition of endogenous CENH3 mainly during G2 phase could explain why CENH3 increases much less than DNA content with endopolyploidy level. Either centromeric regions retain gaps free of (complete) nucleosomes from replication until deposition of *A. thaliana* CENH3 during mid or late G2 or a specific mark leads to substitution of H3 or H3-containing nucleosomes by CENH3 or CENH3-containing nucleosomes during G2, respectively.

The CENH3 Histone Fold Domain Recognizes Different Centromeric Repeats of the Genus *Arabidopsis*, whereas Field Bean Centromeres Are Not Targeted

According to Cooper and Henikoff (2004), the N-terminal region and the histone fold domain, including the loop1 region of the C-terminal part of CENH3 in *Brassicaceae*, evolve in an adaptive manner and can potentially interact with centromeric DNA. However, as also proposed for *Drosophila* (Vermaak et al., 2002) and for human centromeres (Black et al., 2004), only the C-terminal region of *A. thaliana* CENH3 turned out to be responsible for centromere recognition. Recognition by EYFP-CENH3 of all three centromeric repeat types of *A. lyrata*, inspite of polymorphic N-terminal tails of CENH3 between both species, is in line with an observation of Talbert et al. (2002). These authors described immunostaining of all centromeres of the allotetraploid *A. suecica* (*A. thaliana* × *A. arenosa*), while the centromeres of *A. arenosa* remained undetected with the same antibodies against *A. thaliana* CENH3. Wieland et al. (2004) have shown that yeast CENH3 (Cse4p) can complement the absence of CENP-A in human cells. However, EYFP-CENH3 did not label field bean (*V. faba*) centromeres in transformed hairy roots, and the EYFP fluorescence remained restricted to cytoplasm, suggesting a stronger functional diversity of CENH3 homologs, their carrier systems, and/or their centromeric target sequences among higher plants than between the phylogenetic branch comprising fungi and metazoa.

METHODS

Generation of EYFP-CENH3 Fusion Constructs

The EYFP DNA sequence was amplified with the primer pair 5′-ACCACTAGTATGGTGAGCAAGGGCGAGGAG-3′ and 5′-ACTGGATCCCTTGTACAGCTCGTCCATGCC-3′ from the pWEN18 vector, generating an *Spe*I linker sequence at the 5′ end and a *Bam*HI linker sequence at the 3′ end. The stop codon of EYFP was not included. The amplified fragment was inserted downstream the 35S promoter in the unique *Spe*I and *Bam*HI sites of the p35S-BAM vector (Schmidt, www.dna-cloning-service.de). To generate the p35S:EYFP-CENH3 fusion construct, the CENH3 sequence (HTR12 according to Talbert et al., 2002) of *Arabidopsis thaliana*, ecotype Columbia (Col), was amplified from cDNA obtained by reverse transcription of RNA isolated from flower buds with the primer pair 5′-ATACCCGGGATGGCGAGAACCAAGCATCGC-3′ and 5′-CCGGTCGACTCACCATGGTCTGCCTTTTCC-3′, including an *Xma*I restriction site at the 5′ end and a *Sal*I site at the 3′ end for cloning into the p35S-BAM-EYFP vector in frame with EYFP. The resulting expression cassette, including 35S promoter, EYFP-CENH3, and Nos terminator, was subcloned into the pLH7000 vector containing the phosphinotricine resistance marker (www.dna-cloning-service.de) via the *Sfi*I restriction site. To generate constructs for only N- or C-terminal parts of CENH3 fused with EYFP, the same primers as for full-length CENH3 (with an *Xma*I site as forward primer for the N terminus and a *Sal*I site as reverse primer for the C terminus) and additional primers (reverse for the N terminus 5′-ATCGTCGACTCATCGTGGCATAGCCTGTCT-3′, including a *Sal*I site and forward for the C terminus 5′-TTACCCGGGGGCTCACAGAAGAAGTCTTATC-3′, including an *Xma*I restriction site) were used. The resulting PCR fragments were cloned into the same vectors as above.

Plant Transformation, Culture Conditions, and Analysis of EYFP Expression in Vivo

Plants of *A. thaliana* accession Col were transformed according to the flower-dip method (Bechtold et al., 1993). Transgenic EYFP-CENH3–containing progeny were selected after surface sterilization of seeds on Murashige and Skoog medium (Murashige and Skoog, 1962) containing 8 mg/L of phosphinotricine. Growth conditions in a cultivation room were 20°C 16 h light/18°C 8 h dark.

The 35S:EYFP-CENH3 plasmid was also used for particle bombardment of *Arabidopsis lyrata* seedlings grown on Murashige and Skoog plates (Schenk et al., 1998). Transient transformation was performed with 5 mg of plasmid DNA on 25-mg gold particles using a PDS-1000/HE system according to manufacturer's instructions (Bio- Rad). After bombardment, seedlings were incubated for 16 h under standard light/dark conditions prior to EYFP localization via fluorescence microscopy. *Vicia faba* hairy roots transgenic for EYFP-CENH3 were obtained as described (Neumann et al., 1998) except that the *Agrobacterium tumefaciens* strain carried the EYFP-CENH3 vector in addition to the wild-type plasmid pRiA4. The hairy roots originating from cells cotransformed by both plasmids were selected based on their continuous growth on hormone-free medium supplemented with 10 mg/L phosphinotricine. EYFP fluorescence was examined either in vivo or after fixation of root tips in 4% formaldehyde for 10 min at 4°C.

For in vivo EYFP analysis, 7- to 10-d-old seedlings were counterstained with DAPI (1 μg/mL) and placed on slides in a drop of water.

Isolation and Flow Sorting of Nuclei

For the isolation of leaf nuclei, plants were grown in soil in a cultivation room (see above). Leaves were fixed in 4% formaldehyde in Tris buffer (10 mM Tris, 10 mM Na_2EDTA, and 100 mM Triton X-100, pH 7.5) for 20 min. Nuclei were isolated, stained with DAPI (1 μg/mL), and processed for flow sorting according to their fluorescence intensity reflecting the DNA content as described (Jasencakova et al., 2000). Approximately 1000 nuclei of each fraction were sorted onto microscopy slides into a drop containing 100 mM Tris, 50 mM KCl, 2 mM $MgCl_2$, 0.05% Tween 20, and 5% sucrose, air-dried, and used for immunolabeling and/or FISH or stored at −20°C. For isolation of nuclei from roots and leaves, seeds of *A. thaliana* wild-type accession Col and EYFP-CENH3 transgenic plants were germinated in Petri dishes on wet filter paper or on agar medium for 5 to 6 d at room temperature. For flow cytometric measurements of the relative fluorescence intensity of EYFP-CENH3, nuclei were isolated from unfixed leaves or roots. Flow cytometry was performed on the flow sorter FACSAria (BD Biosciences) equipped with a 407- and 488-nm laser for excitation of DAPI and EYFP, respectively. DAPI was measured at 450 nm and EYFP at 530 nm.

Chromosome Preparation

Seeds of the wild type and transformed *A. thaliana* were germinated in Petri dishes on wet filter paper for 3 d at room temperature. Seedlings were fixed for 20 min with ice-cold 4% (w/v) paraformaldehyde in MTSB buffer (50 mM PIPES, 5 mM $MgSO_4$, and 5 mM EGTA, pH 6.9). After

washing 3 × 10 min in MTSB, the seedlings were digested at 37°C for 10 min with a PCP enzyme mixture (2.5% pectinase, 2.5% cellulase Onozuka R-10, and 2.5% Pectolyase Y-23 [w/v] dissolved in MTSB). After washing 3 × 10 min in MTSB, root tips were squashed in a drop of MTSB buffer. After freezing in liquid nitrogen, the cover slips were removed and the slides were immediately transferred into MTSB. Meiotic chromosomes were prepared from flower buds using the same procedure with 40 min of digestion in PCP.

Immunostaining and FISH

Immunostaining of nuclei/chromosomes was performed as described (Jasencakova et al., 2000). EYFP-CENH3 was detected with rabbit polyclonal antisera against GFP (1:500; BD Biosciences) and goat anti-rabbit Cy3 (1:100; Sigma-Aldrich). Endogenous CENH3 was detected using antibodies against *A. thaliana* CENH3 (1:500) and goat anti-rabbit rhodamine (1:100; Jackson Immuno Research Laboratories).

FISH on slides with sorted and squashed nuclei was performed according to Lysak et al. (2006). As probe, pAL harboring the ~180-bp centromere- specific repeat (Martinez-Zapater et al., 1986) was labeled with digoxigenin-dUTP by PCR with sequence-specific primers. The FISH signals were detected using mouse anti-Dig (1:250; Roche) and goat anti-mouse Alexa 488 (1:200; Molecular Probes). For colocalization of CENH3 immunosignals with pAL FISH signals, immunostaining and FISH were performed subsequently; after immunostaining, nuclei were fixed in 4% paraformaldehyde/3.6% sucrose.

Extraction of Total Protein from Flower Buds and Protein Gel Blot Analysis

Plant material (100 mg) was ground under liquid nitrogen and suspended in 500 μL solubilization buffer (56 mM Na_2CO_3, 56 mM dithiothreitol, 2% SDS, 12% sucrose, and 2 mM EDTA). After 15 min of incubation at 70°C, cell debri was removed by centrifugation. Protein concentration was determined according to Bradford (1976). Protein samples were separated by SDS-PAGE in 12.5% polyacrylamide gels according to Laemmli (1970). After blotting, membranes were reversibly stained with 1% ponceau red. Membranes were incubated for 12 h at 10°C in TBS and 3% low-fat milk containing anti-CENH3, anti-GFP, or the secondary antibodies. Secondary anti-rabbit (Bio-Rad) antibodies conjugated to horseradish peroxidase were used to visualize immunocomplexes by an enhanced chemiluminescence detection kit (Bio-Rad) according to manufacturer's instructions.

Microscopy Analysis, Processing of Images, and Statistics

Images were acquired under identical conditions, ensuring that the strongest signal was below the saturation level, using a Zeiss epifluorescence microscope (Axiophot) equipped with ×25/0.80 and ×100/1.4 plan apochromat objectives and a three-chip CCD Sony color camera (DXC-950P). The microscope was integrated into a Digital Optical 3D Microscope system (Schwertner) to generate 3D extended focus images and stacks of optical sections through the specimens as the basis for fluorescence intensity as well as for size measurements of signals and nuclei along the *x*, *y*, and *z* axes. Measurement of speckle intensities from single optical sections of the 3D stacks was performed using TINA 2.0 software. An intensity threshold was set to computationally subtract the background pixels from the image. The corrected sum of gray level values of all signals within the nucleus was used to infer the CENH3 content.

Nuclear and signal volumes were calculated according to the formula $V = xyz\ \pi/6$ and presented as mean values ± SE. Statistical calculations were made using SigmaStat version 2.0 statistical software. Different groups of measurements were compared using one-way analysis of variance and subsequently the Tukey test. P values are given for significance estimation.

Accession Numbers

Sequence data from this article can be found in the GenBank/EMBL data libraries under the following accession numbers: At CENH3 (At1g01370), Aly CENH3 (AY612791), and At HistoneH3 (At4g40040).

ACKNOWLEDGMENTS

This article is dedicated to Ulrich Wobus on the occasion of his 65th birthday. We thank Paul Talbert for providing antibodies against *A. thaliana* CENH3, Andrea Kunze and Jana Latalova for technical assistance, Armin Meister for help with statistics, Alice Navratilova for help with examination of field bean hairy root cultures, Rigomar Rieger and Andreas Houben for critical reading of the manuscript, and Alexandre Berr and Ales Pecinka for helpful discussions. This work was supported by grants from the Deutsche Forschungsgemeinschaft to I.S. (Schu 951/9-3) and from the Academy of Sciences of the Czech Republic to J.M. (AVOZ50510513).

Received April 9, 2006; revised August 9, 2006; accepted September 13, 2006; published October 6, 2006.

REFERENCES

Ahmad, K., and Henikoff, S. (2001). Centromeres are specialized replication domains in heterochromatin. J. Cell Biol. **153,** 101–110.

Allshire, R.C. (1997). Centromeres, checkpoints and chromatid cohesion. Curr. Opin. Genet. Dev. **7,** 264–273.

Amor, D.J., and Choo, K.H. (2002). Neocentromeres: Role in human disease, evolution, and centromere study. Am. J. Hum. Genet. **71,** 695–714.

Amor, D.J., Kalitsis, P., Sumer, H., and Choo, K.H. (2004). Building the centromere: From foundation proteins to 3D organization. Trends Cell Biol. **14,** 359–368.

Badie, C., Itzhaki, J.E., Sullivan, M.J., Carpenter, A.J., and Porter, A.C. (2000). Repression of CDK1 and other genes with CDE and CHR promoter elements during DNA damage-induced G(2)/M arrest in human cells. Mol. Cell. Biol. **20,** 2358–2366.

Bechtold, N., Ellis, J., and Pelletier, G. (1993). In planta *Agrobacterium*-mediated gene transfer by infiltration of adult *Arabidopsis thaliana* plants. C. R. Acad. Sci. Life Sci. **316,** 1194–1199.

Berr, A., Pecinka, A., Meister, A., Kreth, G., Fuchs, J., Blattner, F.R., Lysak, M., and Schubert, I. (2006). Chromosome arrangement and nuclear architecture but not centromeric sequences are conserved between *Arabidopsis thaliana* and *A. lyrata*. Plant J., in press.

Black, B., Foltz, E., Chakravarthy, D.R., Luger, S., Woods, K., Jr, V.L., and Cleveland, D.W. (2004). Structural determinants for generating centromeric chromatin. Nature **430,** 578–582.

Blower, M.D., and Karpen, G.H. (2001). The role of *Drosophila* CID in kinetochore formation, cell-cycle progression and heterochromatin interactions. Nat. Cell Biol. **3,** 730–739.

Blower, M.D., Sullivan, B.A., and Karpen, G.H. (2002). Conserved organization of centromeric chromatin in flies and humans. Dev. Cell **2,** 319–330.

Bradford, M.M. (1976). A rapid and sensitive method for the quantitation of microgram quantities of protein utilizing the principle of protein-dye binding. Anal. Biochem. **72,** 248–254.

Brodsky, W.Y., and Uryvaeva, I.V. (1977). Cell polyploidy: Its relation to tissue growth and function. Int. Rev. Cytol. **50,** 275–332.

Chen, E.S., Saitoh, S., Yanagida, M., and Takahashi, K. (2003). A cell cycle-regulated GATA factor promotes centromeric localization of CENP-A in fission yeast. Mol. Cell **11,** 175–187.

Choo, K.H.A. (1997). The Centromere. (Oxford, UK: Oxford University Press).

Cooper, J.L., and Henikoff, S. (2004). Adaptive evolution of the histone fold domain in centromeric histones. Mol. Biol. Evol. **21,** 1712–1718.

D'Amato, F. (1989). Polyploidy in cell differentiation. Caryologia **42,** 183–211.

D'Amato, F. (1998). Chromosome endoreduplication in growth and development. In Plant Cell Proliferation and Its Regulation in Growth and Development, J.A. Bryant and D. Chiatante, eds (Chichester, UK: Wiley & Sons), pp. 153–166.

Fang, Y., and Spector, D.L. (2005). Centromere positioning and dynamics in living *Arabidopsis* plants. Mol. Biol. Cell **16,** 5710–5718.

Farr, C.J. (2004). Centromeres, kinetochores and the segregation of chromosomes. Foreword. Chromosome Res. **12,** 517–520.

Han, F., Lamb, J.C., and Birchler, J.A. (2006). High frequency of centromere inactivation resulting in stable dicentric chromosomes of maize. Proc. Natl. Acad. Sci. USA **103,** 3238–3243.

Henikoff, S., and Dalal, Y. (2005). Centromeric chromatin: What makes it unique? Curr. Opin. Genet. Dev. **15,** 177–184.

Heun, P., Erhardt, S., Blower, M.D., Weiss, S., Skora, A.D., and Karpen, G.H. (2006). Mislocalization of the *Drosophila* centromere-specific histone CID promotes formation of functional ectopic kinetochores. Dev. Cell **10,** 303–315.

Houben, A., and Schubert, I. (2003). DNA and proteins of plant centromeres. Curr. Opin. Plant Biol. **6,** 554–560.

Howman, E.V., Fowler, K.J., Newson, A.J., Redward, S., MacDonald, A.C., Kalitsis, P., and Choo, K.H. (2000). Early disruption of centromeric chromatin organization in centromere protein A (Cenpa) null mice. Proc. Natl. Acad. Sci. USA **97,** 1148–1153.

Irvine, D.V., Amor, D.J., Perry, J., Sirvent, N., Pedeutour, F., Choo, K.H., and Saffery, R. (2004). Chromosome size and origin as determinants of the level of CENP-A incorporation into human centromeres. Chromosome Res. **12,** 805–815.

Ishida, S., Huang, E., Zuzan, H., Spang, R., Leone, G., West, M., and Nevins, J.R. (2001). Role for E2F in control of both DNA replication and mitotic functions as revealed from DNA microarray analysis. Mol. Cell. Biol. **21,** 4684–4699.

Jasencakova, Z., Meister, A., Walter, J., Turner, B.M., and Schubert, I. (2000). Histone H4 acetylation of euchromatin and heterochromatin is cell cycle dependent and correlated with replication rather than with transcription. Plant Cell **12,** 2087–2100.

Jin, W., Melo, J.R., Nagaki, K., Talbert, P.B., Henikoff, S., Dawe, R.K., and Jiang, J. (2004). Maize centromeres: Organization and functional adaptation in the genetic background of oat. Plant Cell **16,** 571–581.

Karpen, G.H., and Allshire, R.C. (1997). The case for epigenetic effects on centromere identity and function. Trends Genet. **13,** 489–496.

Laemmli, U.K. (1970). Cleavage of structural proteins during the assembly of the head of bacteriophage T4. Nature **227,** 680–685.

Lysak, M., Fransz, P., and Schubert, I. (2006). Cytogenetic analyses of *Arabidopsis.* In Arabidopsis Protocols, 2nd ed., J. Salinas and J.J. Sanchez-Serrano, eds (Totowa, NJ: Humana Press), pp. 173–186.

Maggert, K.A., and Karpen, G.H. (2001). The activation of a neocentromere in *Drosophila* requires proximity to an endogenous centromere. Genetics **158,** 1615–1628.

Malik, H.S., and Henikoff, S. (2002). Conflict begets complexity: The evolution of centromeres. Curr. Opin. Genet. Dev. **12,** 711–718.

Martinez-Zapater, J.M., Estelle, M.A., and Somerville, C.R. (1986). A highly repeated DNA sequence in *Arabidopsis thaliana.* Mol. Gen. Genet. **204,** 417–423.

Mellone, B.G., and Allshire, R.C. (2003). Stretching it: Putting the CEN(P-A) in centromere. Curr. Opin. Genet. Dev. **13,** 191–198.

Murashige, T., and Skoog, F. (1962). A revised medium for rapid growth and bioassays with tobacco tissue cultures. Physiol. Plant **15,** 473–497.

Nagaki, K., Talbert, P.B., Zhong, C.X., Dawe, R.K., Henikoff, S., and Jiang, J. (2003). Chromatin immunoprecipitation reveals that the 180-bp satellite repeat is the key functional DNA element of *Arabidopsis thaliana* centromeres. Genetics **163,** 1221–1225.

Nagl, W. (1978). Endopolyploidy and Polyteny in Differentiation and Evolution. (Amsterdam: North Holland Publishing).

Nasuda, S., Hudakova, S., Schubert, I., Houben, A., and Endo, T.R. (2005). Stable barley chromosomes without centromeric repeats. Proc. Natl. Acad. Sci. USA **102,** 9842–9847.

Neumann, P., Lysak, M., Dolezel, J., and Macas, J. (1998). Isolation of chromosomes from *Pisum sativum* L. hairy root cultures and their analysis by flow cytometry. Plant Sci. **137,** 205–215.

Nicklas, R.B. (1997). How cells get the right chromosomes. Science **275,** 632–637.

Polager, S., Kalma, Y., Berkovich, E., and Ginsberg, D. (2002). E2Fs up-regulate expression of genes involved in DNA replication, DNA repair and mitosis. Oncogene **21,** 437–446.

Ren, B., Cam, H., Takahashi, Y., Volkert, T., Terragni, J., Young, R.A., and Dynlacht, B.D. (2002). E2F integrates cell cycle progression with DNA repair, replication, and G(2)/M checkpoints. Genes Dev. **16,** 245–256.

Schenk, P.M., Elliott, A.R., and Manners, J.M. (1998). Assessment of transient gene expression in plant tissue using the green fluorescent protein as a reference. Plant Mol. Biol. Rep. **16,** 313–322.

Schubert, V., Klatte, M., Pecinka, A., Meister, A., Jasencakova, Z., and Schubert, I. (2006). Sister chromatids are often incompletely aligned in meristematic and endopolyploid interphase nuclei of *Arabidopsis thaliana.* Genetics **172,** 467–475.

Shelby, R.D., Monier, K., and Sullivan, K.F. (2000). Chromatin assembly at kinetochores is uncoupled from DNA replication. J. Cell Biol. **151,** 1113–1118.

Shelby, R.D., Vafa, O., and Sullivan, K.F. (1997). Assembly of CENP-A into centromeric chromatin requires a cooperative array of nucleosomal DNA contact sites. J. Cell Biol. **136,** 501–513.

Takahashi, K., Chen, E.S., and Yanagida, M. (2000). Requirement of Mis6 centromere connector for localizing a CENP-A-like protein in fission yeast. Science **288,** 2215–2219.

Takahashi, K., Takayama, Y., Masuda, F., Kobayashi, Y., and Saitoh, S. (2005). Two distinct pathways responsible for the loading of CENP-A to centromeres in the fission yeast cell cycle. Philos. Trans. R. Soc. Lond. B Biol. Sci. **360,** 595–606.

Talbert, P.B., Masuelli, R., Tyagi, A.P., Comai, L., and Henikoff, S. (2002). Centromeric localization and adaptive evolution of an *Arabidopsis* histone H3 variant. Plant Cell **14,** 1053–1066.

Vafa, O., and Sullivan, K.F. (1997). Chromatin containing CENP-A and alpha-satellite DNA is a major component of the inner kinetochore plate. Curr. Biol. **7,** 897–900.

Van Hooser, A.A., Ouspenski, I.I., Gregson, H.C., Starr, D.A., Yen, T.J., Goldberg, M.L., Yokomori, K., Earnshaw, W.C., Sullivan, K.F., and Brinkley, B.R. (2001). Specification of kinetochore-forming chromatin by the histone H3 variant CENP-A. J. Cell Sci. **114,** 3529–3542.

Vermaak, D., Hayden, H.S., and Henikoff, S. (2002). Centromere targeting element within the histone fold domain of Cid. Mol. Cell. Biol. **22,** 7553–7561.

Warburton, P.E., Cooke, C.A., Bourassa, S., Vafa, O., Sullivan, B.A., Stetten, G., Gimelli, G., Warburton, D., Tyler-Smith, C., Sullivan, K.F., Poirier, G.G., and Earnshaw, W.C. (1997). Immunolocalization of CENP-A suggests a distinct nucleosome structure at the inner kinetochore plate of active centromeres. Curr. Biol. **7,** 901–904.

Wieland, G., Orthaus, S., Ohndorf, S., Diekmann, S., and Hemmerich, P. (2004). Functional complementation of human centromere protein A (CENP-A) by Cse4p from *Saccharomyces cerevisiae.* Mol. Cell. Biol. **24,** 6620–6630.

Zhong, C.X., Marshall, J.B., Topp, C., Mroczek, R., Kato, A., Nagaki, K., Birchler, J.A., Jiang, J., and Dawe, R.K. (2002). Centromeric retroelements and satellites interact with maize kinetochore protein CENH3. Plant Cell **14,** 2825–2836.